

# Characterization of the Substituted *N*-Triazole Oxindole TROX-1, a Small-Molecule, State-Dependent Inhibitor of Ca<sub>v</sub>2 Calcium Channels

Andrew M. Swensen,<sup>1</sup> James Herrington,<sup>2</sup> Randal M. Bugianesi, Ge Dai, Rodolfo J. Haedo,<sup>3</sup> Kevin S. Ratliff,<sup>4</sup> McHardy M. Smith, Vivien A. Warren,<sup>5</sup> Stephen P. Arneric,<sup>4</sup> Cyrus Eduljee, David Parker, Terrance P. Snutch, Scott B. Hoyt, Clare London, Joseph L. Duffy, Gregory J. Kaczorowski,<sup>6</sup> and Owen B. McManus

Departments of Ion Channels (A.M.S., J.H., R.M.B., G.D., R.J.H., K.S.R., M.M.S., V.A.W., O.B.M) and Medicinal Chemistry (S.B.H., C.L., J.L.D.), Merck Research Laboratories, Rahway, New Jersey; and Zalicus Pharmaceuticals, Vancouver, British Columbia, Canada (S.P.A., C.E., D.P., T.P.S.)

Received August 10, 2011; accepted December 21, 2011

## ABSTRACT

Biological, genetic, and clinical evidence provide validation for N-type calcium channels (Ca<sub>v</sub>2.2) as therapeutic targets for chronic pain. A state-dependent Ca<sub>v</sub>2.2 inhibitor may provide an improved therapeutic window over ziconotide, the peptidyl Ca<sub>v</sub>2.2 inhibitor used clinically. Supporting this notion, we recently reported that in preclinical models, the state-dependent Ca<sub>v</sub>2 inhibitor (3*R*)-5-(3-chloro-4-fluorophenyl)-3-methyl-3-(pyrimidin-5-ylmethyl)-1-(1*H*-1,2,4-triazol-3-yl)-1,3-dihydro-2*H*-indol-2-one (TROX-1) has an improved therapeutic window compared with ziconotide. Here we characterize TROX-1 inhibition of Cav2.2 channels in more detail. When channels are biased toward open/inactivated states by depolarizing the membrane potential under voltage-clamp electrophysiology, TROX-1 inhibits Ca<sub>v</sub>2.2 channels with an IC<sub>50</sub> of 0.11 μM. The voltage dependence of Ca<sub>v</sub>2.2 inhibition was examined using automated electrophysiology. TROX-1 IC<sub>50</sub> values were 4.2, 0.90, and 0.36 μM

at -110, -90, and -70 mV, respectively. TROX-1 displayed use-dependent inhibition of Ca<sub>v</sub>2.2 with a 10-fold IC<sub>50</sub> separation between first (27 μM) and last (2.7 μM) pulses in a train. In a fluorescence-based calcium influx assay, TROX-1 inhibited Ca<sub>v</sub>2.2 channels with an IC<sub>50</sub> of 9.5 μM under hyperpolarized conditions and 0.69 μM under depolarized conditions. Finally, TROX-1 potency was examined across the Ca<sub>v</sub>2 subfamily. Depolarized IC<sub>50</sub> values were 0.29, 0.19, and 0.28 μM by manual electrophysiology using matched conditions and 1.8, 0.69, and 1.1 μM by calcium influx for Ca<sub>v</sub>2.1, Ca<sub>v</sub>2.2, and Ca<sub>v</sub>2.3, respectively. Together, these in vitro data support the idea that a state-dependent, non-subtype-selective Ca<sub>v</sub>2 channel inhibitor can achieve an improved therapeutic window over the relatively state-independent Ca<sub>v</sub>2.2-selective inhibitor ziconotide in preclinical models of chronic pain.

## Introduction

The Ca<sub>v</sub>2 subfamily of voltage-dependent calcium channels serves a critical role in the nervous system. This subfamily consists of Ca<sub>v</sub>2.1 (P/Q-type), Ca<sub>v</sub>2.2 (N-type), and Ca<sub>v</sub>2.3 (R-type) channels. These calcium channels provide the main pathway for voltage-triggered calcium influx and subsequent neurotransmitter release at many synapses. Although all three subfamily members probably contribute to processing nociceptive inputs (Pietrobon, 2005), most drug discovery efforts seeking treatments for pathological pain have focused on the Ca<sub>v</sub>2.2 subtype (Yamamoto and Takahara, 2009).

There is extensive evidence to support Ca<sub>v</sub>2.2 as a target for chronic pain treatment. Ca<sub>v</sub>2.2 channels are highly ex-

A.M.S. and J.H. contributed equally to this work.

A.M.S., J.H., R.M.B., G.D., R.J.H., K.S.R., M.M.S., V.A.W., S.B.H., C.L., J.L.D., G.J.K., and O.B.M. are present or former employees of Merck Research Laboratories and may hold stock or stock options in Merck and Co. S.P.A., C.E., D.P., and T.P.S. are present or former employees in Zalicus Pharmaceuticals and may hold stock or stock options in Zalicus Pharmaceuticals.

<sup>1</sup> Current affiliation: Abbott Neuroscience, Abbott Park, Illinois.

<sup>2</sup> Current affiliation: Biochemical Pharmacology/Small Molecule Drug Discovery, Genentech Research and Early Development, Genentech, Inc., South San Francisco, California.

<sup>3</sup> Current affiliation: Nanion Technologies Inc., North Brunswick, New Jersey.

<sup>4</sup> Current affiliation: Pain/Migraine DHT, Eli Lilly and Company, Indianapolis, Indiana.

<sup>5</sup> Current affiliation: Koltan Pharmaceuticals, New Haven, Connecticut.

<sup>6</sup> Current affiliation: Kanalis Consulting, Edison, New Jersey.

Article, publication date, and citation information can be found at <http://molpharm.aspetjournals.org>.

<http://dx.doi.org/10.1124/mol.111.075226>

**ABBREVIATIONS:** Ca<sub>v</sub>, voltage-gated calcium channel; DMSO, dimethyl sulfoxide; HEK, human embryonic kidney; FLIPR, fluorometric imaging plate reader; TROX-1, (3*R*)-5-(3-chloro-4-fluorophenyl)-3-methyl-3-(pyrimidin-5-ylmethyl)-1-(1*H*-1,2,4-triazol-3-yl)-1,3-dihydro-2*H*-indol-2-one.

pressed in laminae I and II of the spinal cord (Gohil et al., 1994; Westenbroek et al., 1998) and are up-regulated in behavioral pain models (Cizkova et al., 2002; Abbadie et al., 2010). Laminae I and II serve as critical relay points in the transmission of pain information into the central nervous system, where primary nociceptors make synaptic connections with dorsal horn neurons of the spinal cord. Opening of presynaptic Ca<sub>v</sub>2.2 channels in response to depolarization of the primary afferent terminal triggers release of transmitter into the synaptic cleft (Evans et al., 1996). Blocking these Ca<sub>v</sub>2.2 channels with conopeptides attenuates nociception in behavioral models of neuropathic and inflammatory pain (Malmberg and Yaksh, 1995; Scott et al., 2002). Furthermore, Ca<sub>v</sub>2.2 knockout mice display reduced pain sensitivity in a number of pain models (Hatakeyama et al., 2001; Kim et al., 2001; Saegusa et al., 2001; Abbadie et al., 2010). Perhaps most convincing are the clinical data from ziconotide, a selective peptide blocker of Ca<sub>v</sub>2.2 channels, which is efficacious in the treatment of chronic pain (Miljanich, 2004).

Although ziconotide provides efficacy against chronic pain, its use is limited by its small therapeutic window and intrathecal route of administration (Miljanich, 2004; Staats et al., 2004). Although some state dependence to ziconotide block is revealed at very negative potentials, within physiological voltage ranges, ziconotide potently inhibits Ca<sub>v</sub>2.2 channels regardless of whether they are in the open, closed, or inactivated state (Stocker et al., 1997; Feng et al., 2003). Small-molecule inhibitors demonstrating strong state-dependent inhibition have been well described for L- and T-type calcium channels (e.g., (Bean, 1984; McDonough and Bean, 1998), and it has been proposed that a state-dependent Ca<sub>v</sub>2.2 inhibitor that preferentially binds to channels in open or inactivated states may provide efficacy with an improved therapeutic window over ziconotide as a result of enhanced activation of Ca<sub>v</sub>2.2 channels in pain conditions (McGivern and McDonough, 2004; Snutch, 2005; Winquist et al., 2005). A number of small-molecule Ca<sub>v</sub>2.2 inhibitors have been described in the literature (for review, see Yamamoto and Takahara, 2009), although detailed mechanistic characterizations of these compounds have not been reported, preventing determination of the value of state-dependent inhibitors in pain treatment.

TROX-1, a substituted *N*-triazole oxindole, is a Ca<sub>v</sub>2.2 inhibitor which exhibits efficacy in a number of animal pain models with a therapeutic window for both cardiovascular and central nervous system side effects (Abbadie et al., 2010). Here we show electrophysiologically that TROX-1 inhibits Ca<sub>v</sub>2.2 channels in both a state-dependent and use-dependent manner. Because state-dependent calcium channel inhibitors can exhibit apparent subtype selectivity owing to different levels of channel inactivation across channel subtypes, we measured the activity of TROX-1 on members of the Ca<sub>v</sub>2 subfamily at various levels of inactivation. When the differences in inactivation are accounted for, TROX-1 is shown to have little molecular subtype selectivity within the Ca<sub>v</sub>2 subfamily. Nevertheless, these results suggest that “functional” selectivity may still be obtained over Ca<sub>v</sub>2 channel isoforms that have more depolarized inactivation-voltage relationships or Ca<sub>v</sub>2 channels that are expressed in cells with more hyperpolarized resting potentials.

## Materials and Methods

**Chemicals.** ((3*R*)-5-(3-Chloro-4-fluorophenyl)-3-methyl-3-(pyrimidin-5-ylmethyl)-1-(1*H*-1,2,4-triazol-3-yl)-1,3-dihydro-2*H*-indol-2-one (TROX-1) was synthesized at Merck Research Labs (Rahway, NJ). Stock solutions of TROX-1 were prepared in DMSO at 10 mM and diluted into assay buffer solutions immediately before use.  $\omega$ -Conotoxin GVIA was obtained from Sigma-Aldrich (St. Louis, MO).

**Cell Lines and Growth Conditions.** Stable HEK293 cell lines expressing human Ca<sub>v</sub>2 calcium channels were described previously (Dai et al., 2008). The Ca<sub>v</sub>2.1 stable line expressed the  $\alpha$ 1A-2 (P-type) splice variant (Hans et al., 1999). The Ca<sub>v</sub>2.2 cell lines (2H8 and CBK) used the long form of  $\alpha$ 1B-1 (Williams et al., 1992). For Ca<sub>v</sub>2.3, the  $\alpha$ 1E-3 splice variant was used (Williams et al., 1994). Each cell line expressed  $\alpha$ 2b $\delta$ -1 and  $\beta$ 3a auxiliary subunits (Williams et al., 1992). After creation of the stable cell lines expressing calcium channels, each line was transfected with cDNA encoding human Kir2.3 (KCNJ4) (Périer et al., 1994) and clonal selection was performed. For electrophysiological experiments, an additional Ca<sub>v</sub>2.2 cell line (bMHN-4) was produced that afforded increased expression levels and improved performance in electrophysiological assays. HEK293 cells were transfected using a dual-vector approach, pcDNA3.1 with long form  $\alpha$ 1B-1 and pBudCE4 with  $\alpha$ 2 $\delta$ -1 and  $\beta$ 3. Clones were selected based on Ca<sub>v</sub>2.2 channel expression using <sup>125</sup>I- $\omega$ -conotoxin-GVIA binding levels and high-expressing clones were further characterized in electrophysiological experiments. Cell lines were cultured at 37°C in Dulbecco's modified Eagle's medium (Mediatech, Inc., Herndon, VA) supplemented with 10% fetal bovine serum (Invitrogen, Carlsbad, CA), penicillin, streptomycin, and glutamine additive (Invitrogen) and appropriate selection antibiotics. Ca<sub>v</sub>2.1 and Ca<sub>v</sub>2.3 cell lines were maintained at 5% CO<sub>2</sub>; Ca<sub>v</sub>2.2 cells were maintained at 10% CO<sub>2</sub>. Ca<sub>v</sub>2.2 and Ca<sub>v</sub>2.3 cell lines were maintained at 30°C for 1 day and Ca<sub>v</sub>2.1 cells for 2 to 3 days before use to enhance expression levels.

**Manual Electrophysiology.** Membrane currents were recorded from the stable HEK293 recombinant cell lines expressing either Ca<sub>v</sub>2.1, Ca<sub>v</sub>2.2 (bMHN-4 cell line), or Ca<sub>v</sub>2.3 channels using the whole-cell patch-clamp technique with a patch-clamp amplifier (EPC 10; HEKA, Port Washington, NY/Axopatch 200B; Molecular Devices, Sunnyvale, CA). Fire-polished borosilicate glass electrodes had resistances from 1 to 3 M $\Omega$  when filled with internal solution. Solutions were applied to cells by bath perfusion via gravity, and flow of solution through the chamber was maintained at all times. Cells exhibiting stable current amplitudes were challenged with compound dissolved in DMSO such that the final DMSO concentration typically did not exceed 0.1% of the external solution and did not affect assay results. For experiments testing the effects of 30  $\mu$ M TROX-1, control and compound solutions had a final DMSO concentration of 0.3%. Compounds were added in escalating concentrations for a minimum of 4 min and percentage inhibition was measured after steady state inhibition was achieved at each concentration. IC<sub>50</sub> values for Ca<sub>v</sub> inhibition were calculated from the fits to the Hill equation [percentage inhibition = 100  $\times$  (1/(1 + (IC<sub>50</sub>/[Compound])<sup>*n*<sub>H</sub></sup>))] with the slope, *n*<sub>H</sub>, fixed to 1. For the initial manual electrophysiology experiments (Figs. 1 and 2), bMHN-4 cells were grown on poly-D-lysine-coated coverglass. The extracellular solution contained 5 mM BaCl<sub>2</sub>, 139 mM CsCl, 1 mM MgCl<sub>2</sub>, 10 mM HEPES, 10 mM glucose, and 10 mM sucrose, pH adjusted to 7.4 with CsOH. The intracellular solution contained 126.5 mM cesium methanesulfonate, 2 mM MgCl<sub>2</sub>, 11 mM EGTA, 10 mM HEPES, 2 mM Na<sub>2</sub>-ATP; osmolarity was adjusted to 295 mOsm using sucrose and pH to 7.3 using CsOH. Leak subtraction was performed using a pulse/number (P/N) protocol set at P/4. The purpose in some manual electrophysiology experiments was to compare inhibition of Ca<sub>v</sub>2.2 channels with inhibition of Ca<sub>v</sub>2.1 and Ca<sub>v</sub>2.3 channels (Fig. 5). As a result of differences in growth patterns between the three cell lines, cells were acutely dissociated from T25 flasks before use. To compensate for lower channel expression levels in the Ca<sub>v</sub>2.1 and Ca<sub>v</sub>2.3 cell lines,

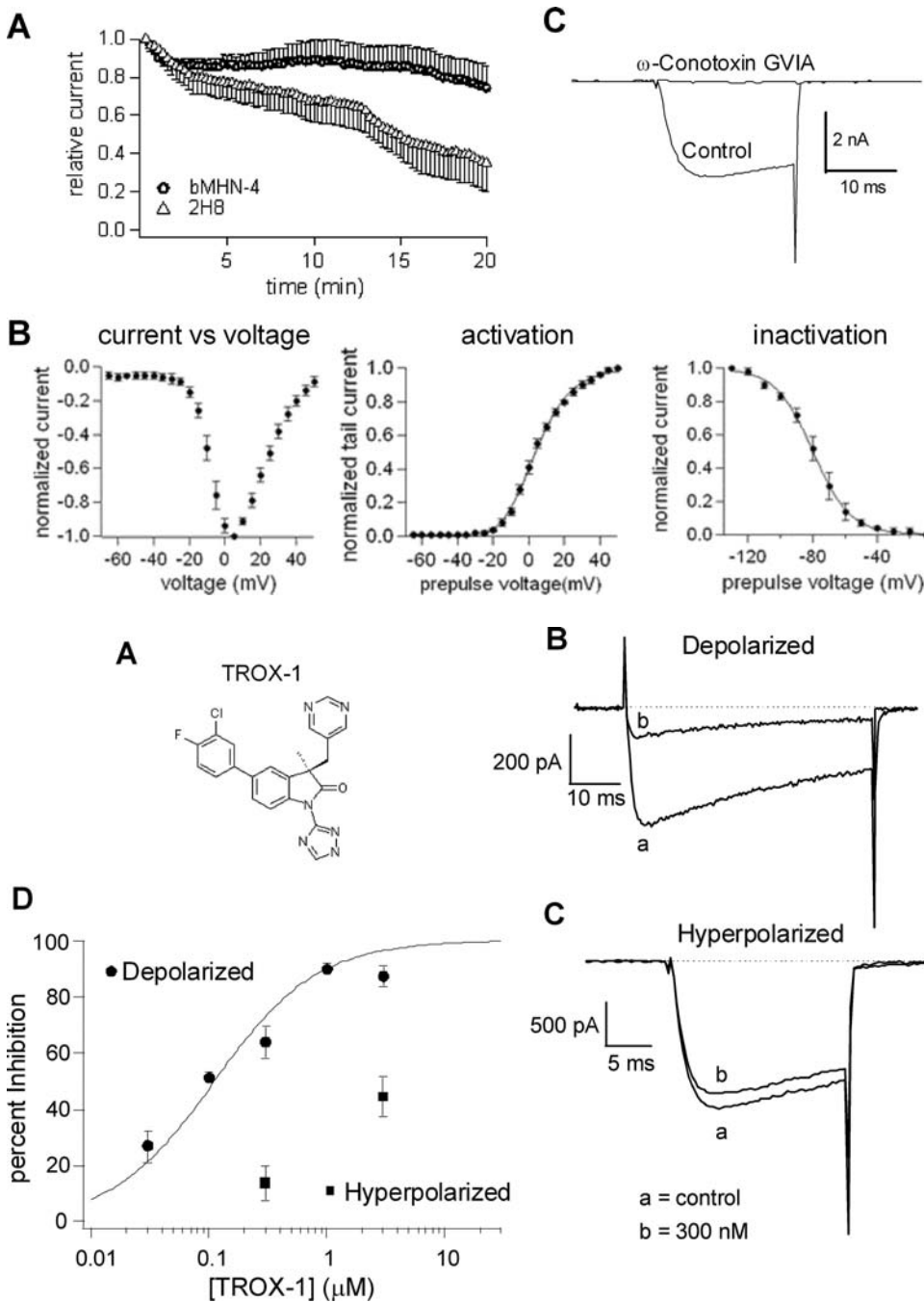


**Fig. 1.** Characterization of bMHN-4  $Ca_v2.2$  cell line. **A**, the bMHN-4  $Ca_v2.2$  cell line ( $n = 14$  cells) showed improved current stability relative to the 2H8 cell line ( $n = 7$  cells). Peak current amplitudes were measured on PatchXpress every 15 s in response to a 50-ms depolarizing step to +10 mV from a holding potential of  $-90$  mV. **B**, characterization of the voltage dependence of bMHN-4 currents. The current versus voltage relationship shows that the peak current amplitudes were elicited near +5 mV ( $n = 5$  cells). Activation ( $n = 4$  cells) and inactivation ( $n = 5$  cells) data were fit with a Boltzmann relationship (see *Materials and Methods* for protocol details). Best fits to the data yielded a half-activation voltage of +4 mV with a slope factor of 9.1 and a half-inactivation voltage of  $-80$  mV with a slope factor of  $-11.5$ . Data are shown as mean  $\pm$  S.E.M. **C**, example illustrating the inhibition of current from the bMHN-4 cell line by 500 nM  $\omega$ -conotoxin GVIA, a  $Ca_v2.2$ -selective peptidyl inhibitor. Current was elicited in response to a 20-ms step to +10 mV from a holding potential of  $-110$  mV.

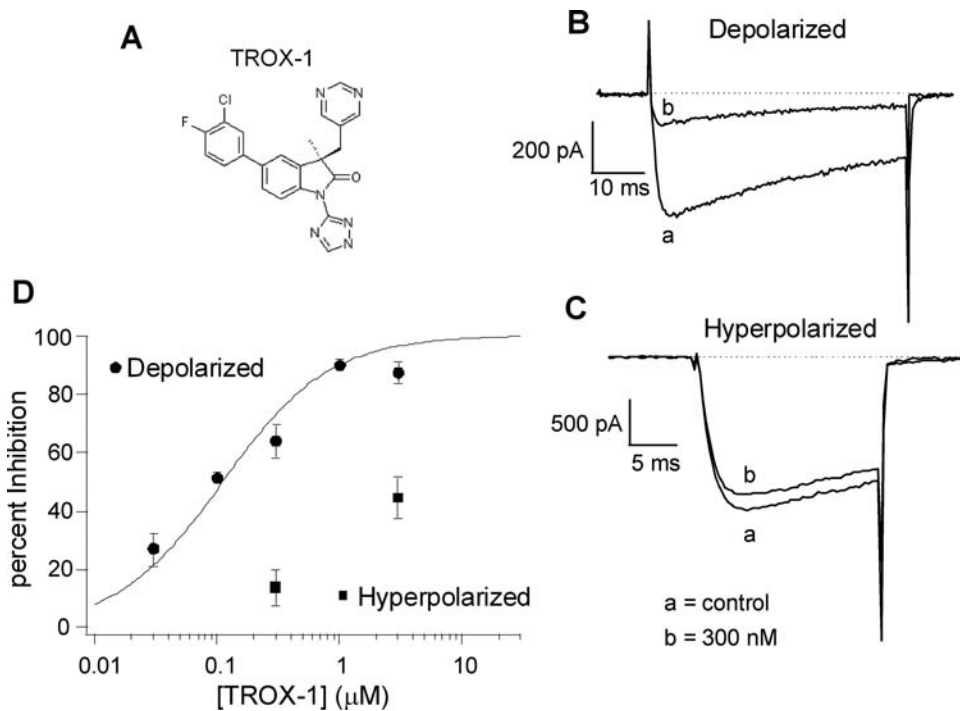


**Fig. 2.** TROX-1 inhibition of  $Ca_v2.2$  current assessed by manual electrophysiology. **A**, chemical structure of the substituted *N*-triazole oxindole, TROX-1. **B** and **C**, representative current traces illustrating the inhibition of  $Ca_v2.2$  current by 300 nM TROX-1 using the depolarized (**B**) and hyperpolarized (**C**) electrophysiological protocols. **D**, concentration-response data for TROX-1 under depolarized ( $n = 3$  cells) and hyperpolarized ( $n = 3-4$  cells) conditions. Voltage protocol details are given in the text. Solid line is a fit of the Hill equation to the data;  $IC_{50}$  value from the fit is given in the text.

a 20 mM barium external solution containing 120 mM NaCl, 20 mM  $BaCl_2$ , 4.5 mM KCl, 0.5 mM  $MgCl_2$ , 10 mM HEPES, and 10 mM glucose, pH adjusted to 7.4 with NaOH, was used for all three cell lines in these experiments. The internal solution for these experiments contained 130 mM CsCl, 10 mM EGTA, 10 mM HEPES, 2 mM  $MgCl_2$ , and 3 mM MgATP, pH adjusted to 7.3 with CsOH.

For generating the current-versus-voltage relationship for the bMHN-4 line, cells were voltage-clamped at  $-100$  mV, and peak currents were measured during 15-ms voltage steps ranging from  $-65$  mV to +50 mV in 5-mV increments. After each step, cells were stepped back down to  $-50$  mV, where deactivation was slow enough to measure tail currents. Normalized tail current measurements were used for generating the activation curve. For the inactivation protocol, cells were voltage-clamped at  $-110$  mV and stepped to voltages ranging from  $-130$  to  $-10$  mV for 10 s (prepulses), and then to +10 mV to elicit current through noninactivated channels. Sweeps

were repeated every 40 s. Control currents were elicited before each prepulse to assure that there was not substantial rundown and that the currents were sufficiently recovered from the previous prepulse. Resulting data were fit to a Boltzmann function:  $y = 1/(1 + \exp((V_h - V)/k))$ , where  $y$  is the current normalized with respect to the maximal current,  $V_h$  is the voltage at which half-activation or inactivation is reached,  $V$  is the voltage, and  $k$  is the slope factor. Data are reported as the mean  $\pm$  S.E.M.

**Automated Electrophysiology using PatchXpress.** PatchXpress is a 16-well whole-cell automated patch clamp device that operates asynchronously with fully integrated fluidics (Molecular Devices). For PatchXpress experiments, cells were grown in T75 culture flasks and dissociated with trypsin 30 to 60 min before use. Capacitance and series resistance compensation were automatically applied and no correction for liquid junction potentials was employed. Leak subtraction was performed using the P/N procedure. Voltage protocols



and the recording of membrane currents were performed using the PatchXpress software/hardware system, and current amplitudes were calculated with DataXpress software. To increase current amplitudes and assay reliability, the same 20 mM barium external solution and corresponding internal solution used for the manual electrophysiology experiments were also used for the PatchXpress experiments. The bMHN-4 cell line was used for the state-dependent assay and the CBK cell line was used for the use-dependent assay. Compounds were added in escalating concentrations (0.3–30 μM) using an integrated pipetter from a 96-well compound plate. Percentage inhibition of peak current by TROX-1 was calculated from the ratio of the current amplitude in the presence and absence of compound. Data are reported as the mean ± S.E.M. IC<sub>50</sub> values for Ca<sub>v</sub>2.2 inhibition were calculated from fits of the Hill equation with the slope fixed to 1.

**Ca<sub>v</sub>2.x Channel Calcium Influx Assays.** Fluorescence-based calcium influx assays as described in Dai et al. (2008) were used to characterize the effects of TROX-1 on Ca<sub>v</sub>2.x channels. Expression of Kir2.3 channels in each cell line allowed control of cell membrane potential through changes in bath potassium concentration (Dai et al., 2008). TROX-1 was incubated with each cell line in the presence of varying levels of bath potassium concentration to assess channel inhibition at different membrane potentials and levels of channel inactivation. After 30 min of compound incubation, channel opening was initiated by 1:1 addition of buffer solution containing 140 mM potassium. Calcium influx signals were measured using a 384 well FLIPR Tetra (Molecular Devices) and calcium indicator dye (Fluo-4). The assay protocol was as follows: Cells were seeded in poly-D-lysine-coated 384-well plates and kept in an incubator overnight at 30°C for Ca<sub>v</sub>2.2 and Ca<sub>v</sub>2.3 cell lines and at 30°C for 2 to 3 days for Ca<sub>v</sub>2.1 cells. Media was removed and cells were washed with 50 μl of Dulbecco's phosphate-buffered saline with calcium and magnesium (Invitrogen). Fifty microliters of 4 μM Fluo-4 (Invitrogen); and 0.02% Pluronic acid F-127 (Invitrogen) prepared in Dulbecco's phosphate-buffered saline supplemented with 10 mM glucose and 10 mM HEPES/NaOH, pH 7.4, was added to each well. Cells were incubated in the dark at 25°C for 60 to 70 min. Dye was removed and cells were washed with 60 μl of potassium prepolarization buffer: *x* mM KCl, 150 – *x* mM NaCl, 0.8 mM CaCl<sub>2</sub>, 1.7 mM MgCl<sub>2</sub>, and 10 mM HEPES, pH 7.2. Thirty microliters of potassium prepolarization buffer was added to each well with or without test compound, and cells were incubated in the dark at 25°C for 30 min. Fluorescence intensity was measured on a FLIPR Tetra instrument (excitation, 480 nm; emission, 535 nm). While fluorescence intensity was continuously read for 40 s, 30 μl of depolarization buffer (140 mM KCl, 10 mM NaCl, 0.8 mM CaCl<sub>2</sub>, 1.7 mM MgCl<sub>2</sub>, and 10 mM HEPES, pH 7.2, which is two times the final assay concentration) was added to each well after 10 s. Peak fluorescent signal intensity was determined, and the amplitude of the peak signal, normalized to baseline, was used to measure channel inhibition by test compounds. Data are reported as the mean ± S.E.M. IC<sub>50</sub> values for Ca<sub>v</sub>2.x inhibition were calculated from fits of the Hill equation to the titration data.

## Results

**Characterization of Ca<sub>v</sub>2.2 Cell Lines.** The Ca<sub>v</sub>2.2 (2H8) cell line used in the calcium influx assay and the Ca<sub>v</sub>2.1 and Ca<sub>v</sub>2.3 cell lines used in both the electrophysiological and influx assays were previously characterized (Dai et al., 2008). For electrophysiological studies involving Ca<sub>v</sub>2.2, a new cell line was created with improved current stability. New cell lines were created using a dual vector approach (see *Materials and Methods*). Clones with high Ca<sub>v</sub>2.2 expression were initially selected using an <sup>125</sup>I-ω-conotoxin-GVIA binding assay and then characterized electrophysiologically on the PatchXpress, an automated patch clamp platform, to select clones with high functional expres-

sion, appropriate biophysical properties, and favorable current stability over time. Under these criteria, the bMHN-4 clone was selected for electrophysiological experiments. The current expressed in the bMHN-4 cell line was larger than that in the original CBK line and, although smaller than that expressed in the 2H8 cell line, was more stable over time (Table 1; Fig. 1A). The bMHN-4 cell line was characterized in more detail by conventional electrophysiology. Maximal current was elicited at ~+5 mV with half-activation occurring at +4 mV and half-inactivation at –80 mV (Fig. 1B). Addition of 500 nM ω-conotoxin-GVIA, a Ca<sub>v</sub>2.2-selective peptide inhibitor, inhibited 99% of the current elicited from voltage steps to +10 mV (*n* = 3 cells; Fig. 1C).

**TROX-1 Inhibits Ca<sub>v</sub>2.2 Currents in a Voltage- and Use-Dependent Manner.** State-dependent inhibition of Ca<sub>v</sub>2.2 channels by TROX-1 was evaluated by applying the compound at two different membrane potentials using the bMHN-4 recombinant cell line. Closed state inhibition was estimated during TROX-1 application at a hyperpolarized membrane potential (–115 mV), where channels are biased toward the closed state; the level of channel inhibition was determined during 20-ms voltage steps to +10 mV every 30 s to elicit current through available, unblocked channels. Potential inhibition of inactivated and/or open channels was explored by applying TROX-1 at more depolarized membrane potentials, with approximately 30% apparent channel inactivation (–75– –85 mV). Peak currents were measured during 50-ms voltage steps to +10 mV every 15 s. For both hyperpolarized and depolarized voltage formats, after stable baseline currents were obtained, compounds were applied by bath perfusion until steady-state inhibition was achieved. Representative current traces for Ca<sub>v</sub>2.2, ± 300 nM TROX-1, are shown for the depolarized (Fig. 2B) and the hyperpolarized (Fig. 2C) assay formats. Using the depolarized protocol, TROX-1 inhibited Ca<sub>v</sub>2.2 in a concentration-dependent manner with an estimated IC<sub>50</sub> of 0.11 μM (Fig. 2D). Under hyperpolarized conditions, where channels are biased toward the closed state, TROX-1 was less potent, blocking only 14 ± 6 and 45 ± 7% of the calcium current at 0.3 and 3 μM, respectively.

The dependence of TROX-1 activity on membrane potential and channel state was further characterized using PatchXpress. As for the manual patch clamp assay, cells were stepped to +10 mV every 15 s to elicit current and evaluate inhibition. The holding potential, however, was varied in 20-mV increments from –110 to –70 mV for different groups of cells. Representative current-versus-time plots and current traces are shown for TROX-1 inhibition of Ca<sub>v</sub>2.2 from holding potentials of –70 mV (Fig. 3A) and –110 mV (Fig. 3B). Similar to the results for manual patch assay, the apparent potency of TROX-1 depended on the hold-

TABLE 1

Comparison of current expression in the CBK, 2H8, and bMHN-4 Ca<sub>v</sub>2.2 stable cell lines as measured by automated electrophysiology. Peak current amplitudes were measured on PatchXpress in response to a 50-ms depolarizing step to +10 mV from a holding potential of –90 mV. Data are reported as mean ± S.E.M.

Cell Line	Current at +10 mV	
	nA	<i>n</i>
CBK	1.6 ± 0.6	8
2H8	5.6 ± 0.7	21
bMHN-4	2.2 ± 0.5	14

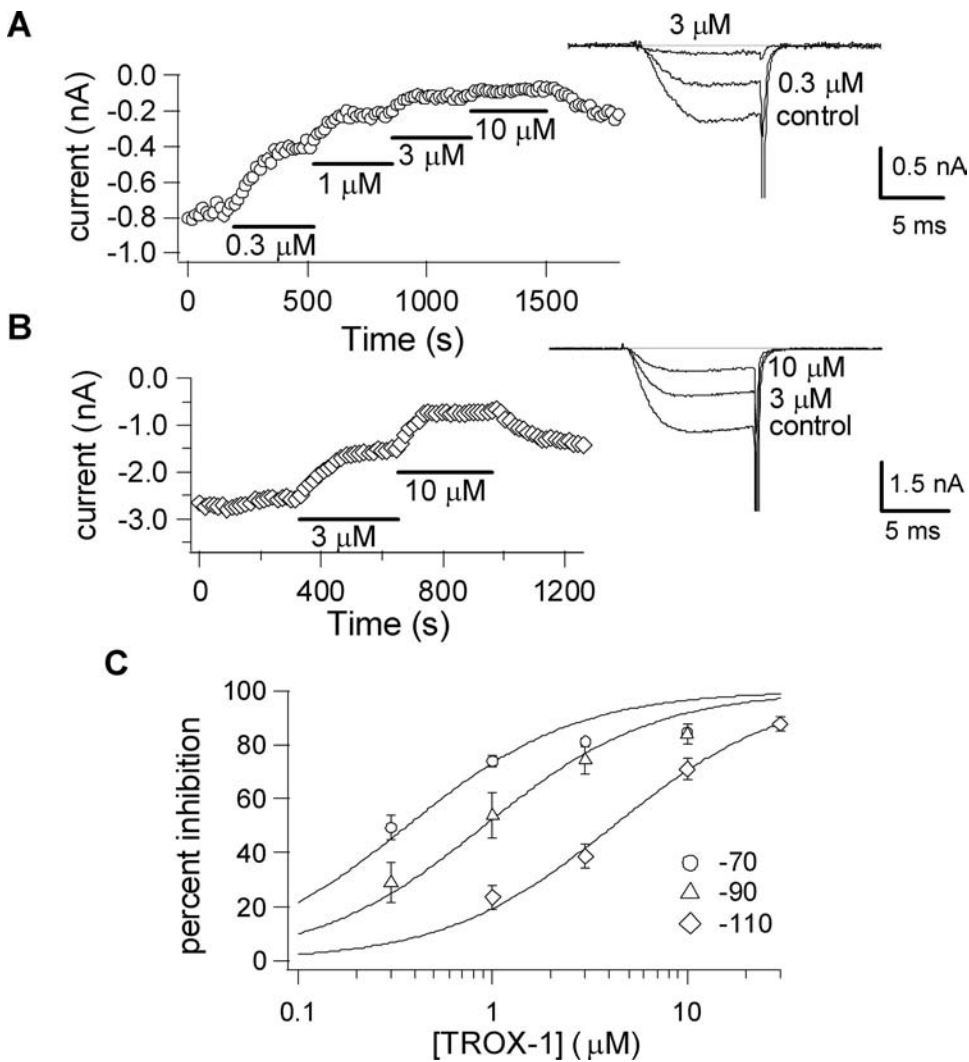


**Fig. 3.** State dependence of TROX-1 inhibition of  $\text{Ca}_v2.2$  channels measured by automated electrophysiology. **A**, plot of the peak inward current versus time for a cell (bMHN-4) recorded on the PatchXpress (left). The solid bars represent when TROX-1 was present in the well at the concentrations shown. The membrane potential was stepped to +10 mV every 15 s from a holding potential of -70 mV. Representative leakage-subtracted currents before and after adding 0.3 and 3  $\mu\text{M}$  TROX-1 are shown at right. **B**, plot of peak inward current versus time (left) for a different cell under conditions identical to those in **A** except that the holding potential was -110 mV. Representative leakage-subtracted currents before and after adding 3 and 10  $\mu\text{M}$  TROX-1 are shown at right. The peak tail current has been truncated for scaling purposes. **C**, plot of the average percentage inhibition of peak inward  $\text{Ca}_v2.2$  current versus the concentration of TROX-1. The solid lines are fits of the Hill equation to the data;  $\text{IC}_{50}$  values from the fits are given in the text. For -70 and -90 mV,  $n = 6$  for each data point. For -110 mV data,  $n = 6$  for 1 and 30  $\mu\text{M}$  and  $n = 8$  for 3 and 10  $\mu\text{M}$ .

ing membrane potential with the  $\text{IC}_{50}$  shifting from 0.36  $\mu\text{M}$  at -70 mV to 4.2  $\mu\text{M}$  at -110 mV (Fig. 3C).

Use-dependent inhibition of  $\text{Ca}_v2.2$  channels expressed in the CBK cell line was examined using PatchXpress. The CBK cell line was chosen because the currents in response to voltage trains were more stable than the currents in 2H8 or bMHN-14 cells. The cause of these stability differences is unclear but may involve differences in channel inactivation across the cell lines. The  $\text{Ca}_v2.2$  currents in CBK cells exhibit a more depolarized, two-component steady-state inactivation curve probably due to limiting expression of  $\beta3a$  (discussed in Dai et al., 2008). CBK cells were voltage clamped at -60 mV, which corresponds to ~80% availability at steady-state, and trains of 20 pulses (25 ms) to +20 mV were applied at a frequency of 2 Hz every 5 min. Representative currents at pulses 1 and 20 under control conditions and in the presence of 3  $\mu\text{M}$  TROX-1 are shown in Fig. 4A. Inspection of the time course of current reduction during the pulse train shows that inhibition mainly develops over the first 10 pulses and has reached steady-state by the 20th pulse (Fig. 4C). The averaged data presented in Fig. 4B illustrates that TROX-1 inhibited the current elicited at pulse 20 more potently ( $\text{IC}_{50}$ , 2.4  $\mu\text{M}$ ) than the current elicited at pulse 1 ( $\text{IC}_{50}$ , 24  $\mu\text{M}$ ), indicating enhanced inhibition of  $\text{Ca}_v2.2$  channels after a train of depolarizing pulses that open and inactivate  $\text{Ca}_v2.2$

channels. Together, these data demonstrate that TROX-1 inhibits  $\text{Ca}_v2.2$  channels in both a voltage- and use-dependent manner and are consistent with state-dependent inhibition of inactivated and/or open channels by TROX-1.

**TROX-1 Inhibits Other Members of the  $\text{Ca}_v2$  Subfamily of Calcium Channels.** In manual electrophysiology experiments, TROX-1 activity was compared across other members of the  $\text{Ca}_v2$  subfamily of calcium channels to assess its selectivity profile. Lower expression levels in the  $\text{Ca}_v2.1$  and  $\text{Ca}_v2.3$  cell lines required an increase in the concentration of the barium charge carrier from 5 (Fig. 2) to 20 mM. TROX-1 activity on  $\text{Ca}_v2.2$  was reassessed using 20 mM barium as the charge carrier to allow for a direct comparison of potency across all three  $\text{Ca}_v2$  subfamily members without concern for potency shifts that might result from differences in the concentration of the charge carrier. TROX-1 inhibition of  $\text{Ca}_v2$  currents was measured using both "hyperpolarized" and "depolarized" voltage formats, as described previously (Dai et al., 2008). In brief, for the hyperpolarized format, cells were voltage-clamped at -100 mV and stepped to +10 mV every 15 s. For the depolarized format, cells were also stepped to +10 mV every 15 s; however, cells were first voltage-clamped at -100 mV to establish a baseline current amplitude and then depolarized to a holding membrane potential, which resulted in ~30% inactivation of the current. For  $\text{Ca}_v2.2$  and

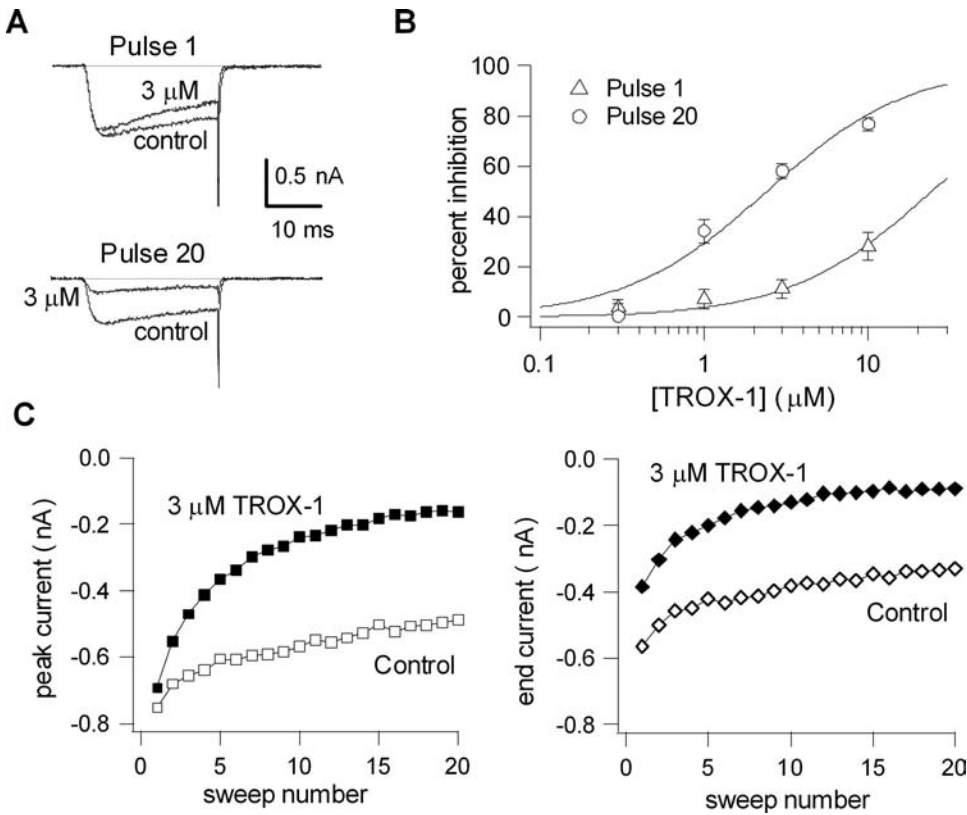


**Fig. 4.** Use-dependent inhibition of Ca<sub>v</sub>2.2 channels by TROX-1. A, representative Ca<sub>v</sub>2.2 currents recorded on the PatchXpress before and after application of 3 μM TROX-1. CBK cells were voltage-clamped at -60 mV, and trains of 20 25-ms pulses to +20 mV were applied at a frequency of 2 Hz every 5 min. Shown are the currents in response to pulse 1 (top) and pulse 20 (bottom) of the train. B, plot of the average percent inhibition of peak inward Ca<sub>v</sub>2.2 current at pulses 1 and 20 versus the concentration of TROX-1. Solid lines are fits of the Hill equation to the data. IC<sub>50</sub> values from the fits are given in the text. For each data point  $n = 5$ . C, plots of peak current (left) and end current amplitude (right) versus sweep number before (open symbols) and after (closed symbols) application of 3 μM TROX-1 for the recording shown in A.

Ca<sub>v</sub> 2.3 channels, this voltage was typically -70 to -75 mV. For the less inactivating Ca<sub>v</sub>2.1 cell line, this voltage was ~-40 mV. Under the hyperpolarized conditions, TROX-1 showed an apparent selectivity for Ca<sub>v</sub>2.2 and Ca<sub>v</sub>2.3 over Ca<sub>v</sub>2.1 (Fig. 5, squares; IC<sub>50</sub> = 37, 1.1, and 1.2 for Ca<sub>v</sub>2.1, Ca<sub>v</sub>2.2, and Ca<sub>v</sub>2.3, respectively). However, when TROX-1 inhibition of Ca<sub>v</sub>2 channels was assessed under depolarized conditions where the channels exhibited similar levels of inactivation, no selectivity was apparent (Fig. 5, circles: IC<sub>50</sub> = 0.29, 0.19, and 0.28 μM for Ca<sub>v</sub>2.1, Ca<sub>v</sub>2.2, and Ca<sub>v</sub>2.3, respectively).

TROX-1 inhibition of Ca<sub>v</sub>2 channels was also examined in a calcium influx assay on a FLIPR with the throughput to assess inhibition of all three subfamily members across a

range of conditions (see Dai et al., 2008). This assay uses Ca<sub>v</sub>2.1, Ca<sub>v</sub>2.2, and Ca<sub>v</sub>2.3 cell lines that coexpress the Kir2.3 inward rectifier potassium current and therefore allows the membrane potential of the cells to be varied by changing the external potassium concentration. Cells were preincubated in potassium prepolarization buffers with variable potassium concentrations, with or without TROX-1, and then channel opening was triggered with a high K<sup>+</sup> depolarization buffer (see *Materials and Methods*). Figure 6 compares TROX-1 inhibition of calcium influx when the preincubation external potassium was relatively low (A; 4 mM), and when the external potassium was higher (B; 14 mM). The top section of each subpanel in Fig. 6 shows example calcium influx data from a row of 24 wells in a 384-well assay plate.

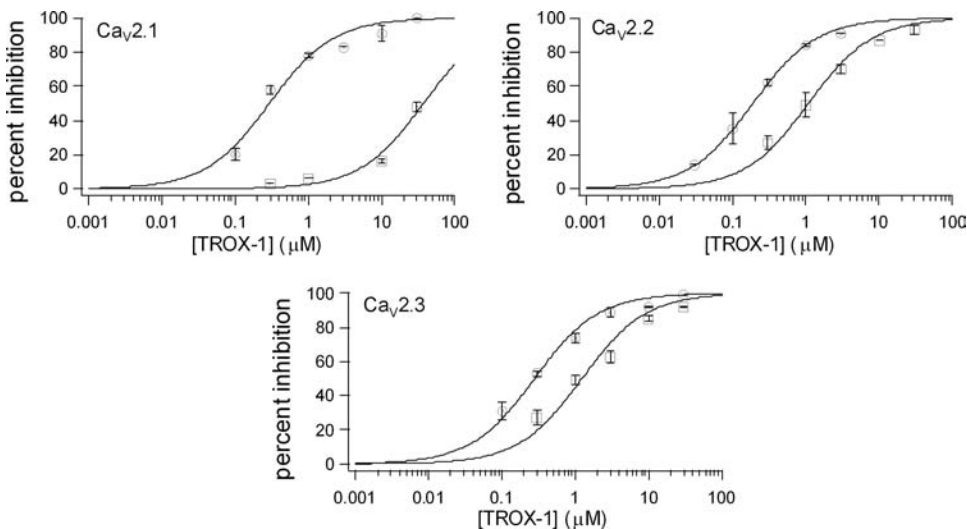


**Fig. 5.** Comparison of TROX-1 inhibition of Ca<sub>v</sub>2.1, Ca<sub>v</sub>2.2, and Ca<sub>v</sub>2.3 current assessed by manual electrophysiology. Using the depolarized voltage format in which Ca<sub>v</sub>2.1, Ca<sub>v</sub>2.2, and Ca<sub>v</sub>2.3 channels were similarly inactivated, TROX-1 inhibited all three Ca<sub>v</sub>2 subfamily members with a similar potency. Although TROX-1 displayed state-dependent inhibition of all three Ca<sub>v</sub>2 subfamily members, TROX-1 inhibition measured using the hyperpolarized voltage format was less potent for Ca<sub>v</sub>2.1 than that observed for Ca<sub>v</sub>2.2 and Ca<sub>v</sub>2.3. Voltage protocol details are given in the text. Solid lines are fits of the Hill equation to the data; IC<sub>50</sub> values from the fits are given in the text. For the depolarized voltage format,  $n = 6, 9,$  and  $7$  cells for Ca<sub>v</sub>2.1, Ca<sub>v</sub>2.2, and Ca<sub>v</sub>2.3, respectively. For the hyperpolarized voltage format,  $n = 5, 5,$  and  $9$  cells for Ca<sub>v</sub>2.1, Ca<sub>v</sub>2.2, and Ca<sub>v</sub>2.3, respectively.



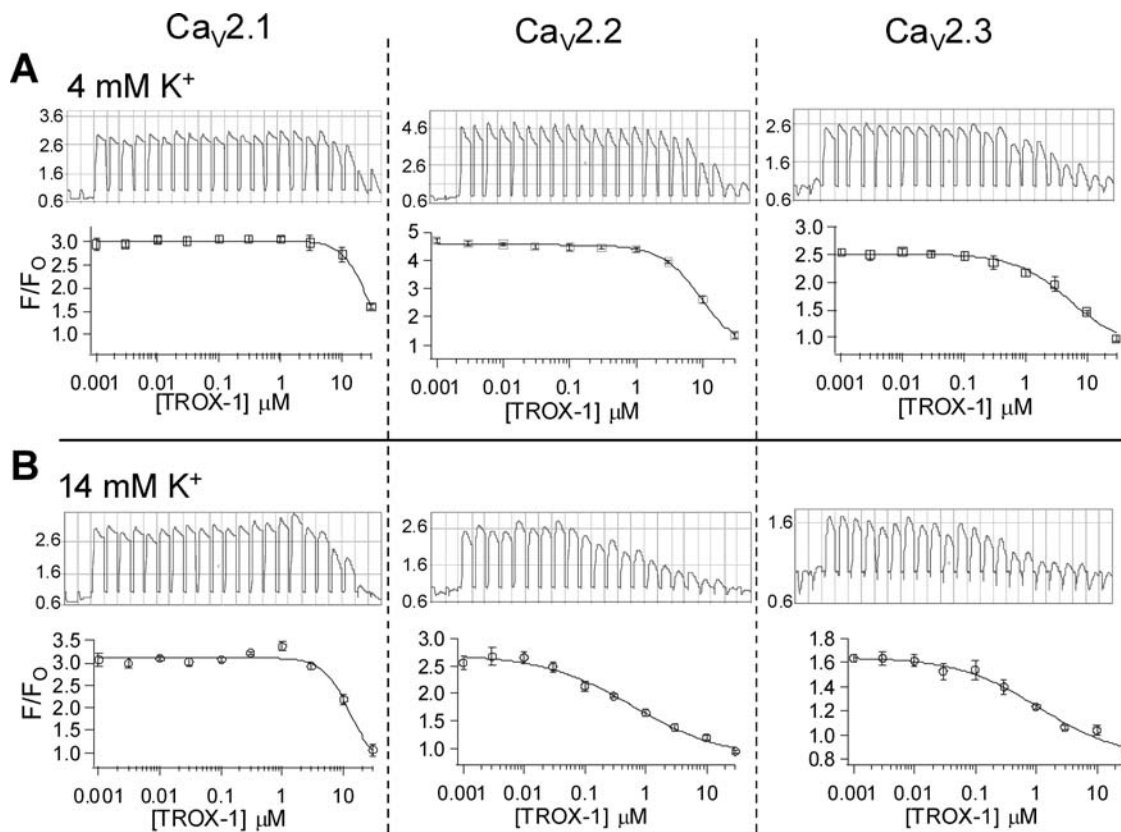


**Fig. 6.** Selectivity and state-dependent inhibition of  $\text{Ca}_v2.1$ ,  $\text{Ca}_v2.2$ , and  $\text{Ca}_v2.3$  channels in a calcium-influx assay. Top, data from a row of 24 wells in a 384-well assay plate showing calcium influx under either hyperpolarized (A, 4 mM  $\text{K}^+$  preincubation) or depolarized (B, 14 mM  $\text{K}^+$  preincubation) conditions followed by a 140 mM  $\text{K}^+$  addition (1:1) to depolarize cells and open channels. The leftmost two wells in each row contained 10  $\mu\text{M}$  concentrations of a nonselective  $\text{Ca}_v2.x$  blocker, the next two wells from the left contained control buffer, and the following wells contained increasing concentrations of TROX-1 in a 10-point titration format in duplicate from 1 nM to 30  $\mu\text{M}$ . Bottom, analysis of TROX-1 concentration-response data for each experiment under hyperpolarized (A) or depolarized (B) conditions. Data are reported as the mean  $\pm$  S.E.M ( $n = 4$ ). Solid lines are fits of the Hill equation to the data;  $\text{IC}_{50}$  values from the fits are given in the text.

The leftmost two wells in each row contain a nonselective  $\text{Ca}_v2$  blocker as a positive control followed by two wells containing control buffer and the remaining wells containing increasing concentrations of TROX-1 in duplicate. Analysis of concentration-response data are shown in the bottom section of each subpanel. With these potassium concentrations,  $\text{Ca}_v2.2$  and  $\text{Ca}_v2.3$  channels show a marked shift in TROX-1 potency between the 4 and 14 mM  $\text{K}^+$  conditions ( $\text{IC}_{50}$  values decreasing from 9.48 to 0.69  $\mu\text{M}$  for  $\text{Ca}_v2.2$  and from 5.13 to 1.09  $\mu\text{M}$  for  $\text{Ca}_v2.3$ ), whereas the shift for  $\text{Ca}_v2.1$  channels was more moderate ( $\text{IC}_{50}$  decreased from 25.6 to 12.4  $\mu\text{M}$ ). A large part of this differential shift between the  $\text{Ca}_v2$  subfamily members is a result of the weaker potency of TROX-1 on  $\text{Ca}_v2.1$ , relative to  $\text{Ca}_v2.2$  and  $\text{Ca}_v2.3$ , under the 14 mM  $\text{K}^+$  condition. Although the three cell lines should be at similar voltages in 14 mM  $\text{K}^+$  (Dai et al., 2008), the fluorescence values from Fig. 6 show that the calcium influx for  $\text{Ca}_v2.2$  and  $\text{Ca}_v2.3$  is reduced in the 14 mM  $\text{K}^+$  condition but relatively unchanged for  $\text{Ca}_v2.1$ . This is consistent with the more depolarized inactivation-voltage relationship of  $\text{Ca}_v2.1$  relative to  $\text{Ca}_v2.2$  and  $\text{Ca}_v2.3$  (see Figs. 1B and 2D; Dai et al., 2008).

To better understand the relationship between calcium channel inactivation and potency, TROX-1 inhibition of  $\text{Ca}_v2.1$ -,  $\text{Ca}_v2.2$ -, and  $\text{Ca}_v2.3$ -mediated calcium influx was examined across a range of external potassium concentrations. The dependence of the calcium signal on external po-

tassium varied across the three  $\text{Ca}_v2$  subfamily members,  $\text{Ca}_v2.1$  being the most right-shifted (Fig. 7, A–C, black open squares). Likewise, the dependence of TROX-1 potency on external potassium varied across the three subfamily members,  $\text{Ca}_v2.1$  again being the most right-shifted (Fig. 7, A–C, colored open symbols). It is noteworthy that if the  $\text{IC}_{50}$  for TROX-1 inhibition is plotted versus the fractional reduction in calcium signal, there is little difference in the potency of TROX-1 across the three  $\text{Ca}_v2$  subfamily members (Fig. 7D). These results suggest that the apparent differences in TROX-1 potencies observed under different assay conditions are simply a reflection of the degree of inactivation between the channels. Taken together, these data show that TROX-1 is a highly state-dependent inhibitor of all three members of the  $\text{Ca}_v2$  subfamily of calcium channels with very little, if any, true molecular selectivity across subtypes.

## Discussion

The results reported here show that the substituted *N*-triazole oxindole TROX-1 is a potent state-dependent inhibitor of human  $\text{Ca}_v2.2$  calcium channels. Measured electrophysiologically under depolarized conditions, TROX-1 inhibits recombinant h $\text{Ca}_v2.2$  currents with an estimated  $\text{IC}_{50}$  of 0.11  $\mu\text{M}$ . However, when cells are hyperpolarized to minimize open and inactivated state inhibition, TROX-1 potency is reduced, blocking only  $45 \pm 7\%$  of the current at 3  $\mu\text{M}$ . These

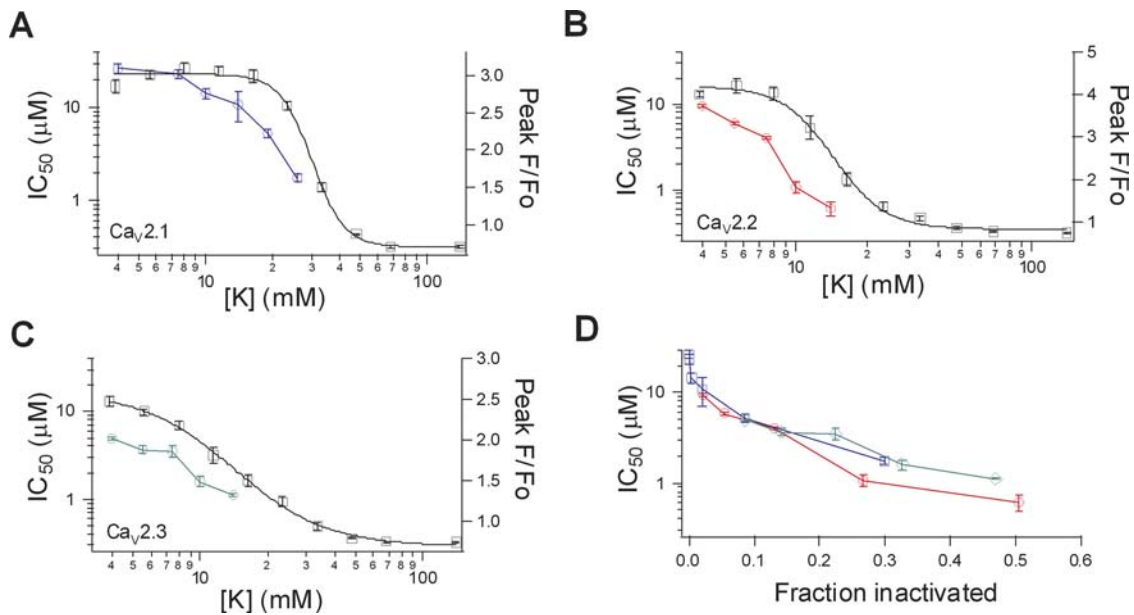


**Fig. 7.** Relationship between TROX-1 potency and calcium channel inactivation for  $Ca_v2.1$ ,  $Ca_v2.2$ , and  $Ca_v2.3$  channels in a calcium-influx assay. A to C, plots of TROX-1  $IC_{50}$  values (colored symbols;  $n = 4$  experiments) and peak fluorescent signal (black squares; one experiment in quadruplicate) versus the preincubation external potassium concentration for  $Ca_v2.1$  (A),  $Ca_v2.2$  (B), and  $Ca_v2.3$  (C). D, plot of TROX-1  $IC_{50}$  values versus the fractional reduction in the peak calcium signal for  $Ca_v2.1$  (blue),  $Ca_v2.2$  (red), and  $Ca_v2.3$  (green).

results are in good agreement with  $IC_{50}$  values for TROX-1 inhibition of native calcium channel currents from dissociated rat DRG neurons under depolarized (0.4  $\mu M$ ) and hyperpolarized (2.6  $\mu M$ ) conditions (Abbadie et al., 2010). The state dependence of TROX-1 inhibition of calcium channels was also observed using a calcium influx assay in which the TROX-1  $IC_{50}$  shifted from 0.69  $\mu M$  under high external potassium (14 mM  $K^+$ , partially inactivated) conditions to 9.48  $\mu M$  under low external potassium (4 mM  $K^+$ ) conditions. This is in reasonable agreement with the 0.27 and  $>10$   $\mu M$  values from Abbadie et al. (2010), which were obtained using a different cell line and with 30 mM  $K^+$  for the high potassium condition. Measured electrophysiologically, Electrophysiologically, TROX-1 also inhibited  $Ca_v2.2$  channels in a use-dependent manner. TROX-1 inhibited  $Ca_v2.2$  current during the 20th pulse of a 2-Hz train approximately 10-fold more potently than during the first pulse of the train.

Because TROX-1 shows selectivity for  $Ca_v2.2$  over  $Ca_v1.2$  (L-type, 18  $\mu M$ ) and  $Ca_v3.1/3.2$  (T-type, 15 and  $>20$   $\mu M$ , respectively) (Abbadie et al., 2010), we also wanted to determine TROX-1 selectivity within the  $Ca_v2$  subfamily. When cells are depolarized to obtain comparable levels of inactivation, TROX-1, measured electrophysiologically, has a similar potency across  $Ca_v2.1$ ,  $Ca_v2.2$ , and  $Ca_v2.3$  calcium channels. However, when cells are voltage-clamped at  $-100$  mV, TROX-1 appears  $>30$ -fold selective for  $Ca_v2.2$  and  $Ca_v2.3$  relative to  $Ca_v2.1$ . It is noteworthy that although  $-100$  mV is near the foot of the inactivation curve for both  $Ca_v2.2$  and  $Ca_v2.3$ , it is  $\sim 60$  mV hyperpolarized from the foot of the inactivation curve for  $Ca_v2.1$  (see Figs. 1B and 2D) (Dai et al., 2008). The apparent difference in potency, therefore, may reflect the fact that the  $Ca_v2.1$  potency at  $-100$  mV better approximates closed-state inhibition. The results from the calcium influx experiments support this interpretation. In the calcium influx assays, the relationship between  $IC_{50}$  and external potassium is shifted to higher potassium concentrations (more depolarized) for  $Ca_v2.1$  relative to  $Ca_v2.2$  and

$Ca_v2.3$  (Fig. 7, A–C). If, however,  $IC_{50}$  values are plotted versus fractional reduction in calcium signal to normalize for channel inactivation, TROX-1 potency is essentially identical for  $Ca_v2.1$ ,  $Ca_v2.2$ , and  $Ca_v2.3$  across a range of inactivation levels (Fig. 7D). These results suggest that TROX-1 is interacting with the inactivated state of the channel, although these data do not exclude other potential mechanisms such as effects on open channels, channel activation, or closed-closed channel state transitions that might occur at depolarized potentials. Although these results indicate that there may be little true molecular selectivity within the  $Ca_v2$  subfamily, TROX-1 could still be functionally selective against less inactivated  $Ca_v2$  calcium channels. This is probably a physiologically relevant consideration, because  $Ca_v2$  inactivation levels are not only modulated by the voltage and activity of the neurons expressing them but also can be dependent on the splice variant (Bourinet et al., 1999; Thaler et al., 2004), coexpressed auxiliary subunit (De Waard and Campbell, 1995), or interacting proteins including synaptic proteins (Bezprozvanny et al., 1995; Zhong et al., 1999; Kiyonaka et al., 2007).

Molecular selectivity can be examined in both the electrophysiological and calcium influx assays by measuring potency under similar levels of inactivation (see also Dai et al., 2008); however, more caution should be taken when comparing the absolute degree of state dependence across the different  $Ca_v2$  assays. The degree of state dependence is determined by comparing the potency under depolarized conditions with the potency under hyperpolarized conditions in which channels are presumed to be largely in the closed state. However, as discussed above for the electrophysiological assay, the potency values in the calcium influx assay under hyperpolarized conditions (low potassium) are probably influenced by the proximity of the cell resting potential to the foot of the inactivation curve.  $Ca_v2.1$  and  $Ca_v2.2$  channels seem largely noninactivated at 4 mM extracellular  $K^+$  in these cell lines because the top of the inactivation curves are



relatively flat (Fig. 7, A and B). The decreasing signal for Ca<sub>v</sub>2.3, however, suggests that it is close to the foot of its inactivation curve and this may contribute to its slightly increased potency in 4 mM K<sup>+</sup> (Fig. 7C) and, therefore, to its reduced apparent state dependence. As a result, the state-dependent measures from these assays are most useful for comparing different compounds on the same channel rather than the same compound across different channels.

There is a tendency for TROX-1 to seem more potent in the electrophysiological assays. This is consistent with that reported for two other Ca<sub>v</sub>2.2 inhibitors assessed in these same assays (Dai et al., 2008) and may be tied to differences between the assay formats. Although the cell membrane potentials in the calcium influx assay are likely to be relatively constant during compound incubation, the cells are depolarized periodically in the electrophysiological assay, which could contribute an additional use-dependent component to the inhibition.

The issue of selectivity within the Ca<sub>v</sub>2 subfamily of calcium channels raises the question of how the individual inhibitory activities on Ca<sub>v</sub>2.1, Ca<sub>v</sub>2.2, and Ca<sub>v</sub>2.3 might influence overall efficacy and safety profiles. Genetic ablation of these channels in mice probably provides only a partial answer. Ca<sub>v</sub>2.3(-/-) mice, for example, have been reported to be resistant to inflammatory pain but otherwise exhibit a predominantly normal phenotype with alterations in glucose metabolism (Saegusa et al., 2000; Wilson et al., 2000; Matsuda et al., 2001). Reports on the role of Ca<sub>v</sub>2.1 channels in pain have been less straightforward with evidence of reduced pain sensitivity in the Ca<sub>v</sub>2.1 knockout mice (Luvisetto et al., 2006) but hypersensitivity using pharmacological blockade of Ca<sub>v</sub>2.1 at supraspinal levels (Knight et al., 2002; Ebersberger et al., 2004). In terms of potential adverse effects, Ca<sub>v</sub>2.1(-/-) mice, which die within 3 to 4 weeks of birth, exhibit ataxia, dystonia, and absence seizures. This phenotype is consistent with human Ca<sub>v</sub>2.1 loss-of-function mutations, which result in episodic ataxia and absence seizures (Pietrobon, 2005). Despite this, the efficacy and safety data of TROX-1 in animal models suggest that an adequate safety window can be obtained with a state-dependent, nonselective Ca<sub>v</sub>2 inhibitor (Abbadie et al., 2010). The therapeutic window for a given compound is likely to depend on both its molecular selectivity and its degree of state dependence. Until additional studies are reported for a range of Ca<sub>v</sub>2.2 inhibitors, the combination of selectivity and state-dependent profiles that best maximize the safety window will remain an open question.

A number of small-molecule Ca<sub>v</sub>2.2 inhibitors have now been reported with various potencies and selectivity profiles (Yamamoto and Takahara, 2009). High-affinity Ca<sub>v</sub>1.2 (L-type) calcium channel inhibitors carry known cardiovascular liabilities, and much effort has focused on developing Ca<sub>v</sub>2.2 inhibitors with selectivity over L-type channels (Zhang et al., 2008; Zamponi et al., 2009; Abbadie et al., 2010). Selectivity against Ca<sub>v</sub>3 (T-type) calcium channels and other Ca<sub>v</sub>2 subfamily members has also been reported but, in general, has been much more limited (Yamamoto and Takahara, 2009). As shown here, for state-dependent inhibitors, it is important to generate selectivity data in assays producing similar degrees of channel inactivation. Furthermore, a more informative and detailed understanding of inhibitor selectivity profiles can be obtained by looking at potencies across a range of

voltages and inactivation levels, particularly for closely related family members, where true molecular selectivity may be more difficult to obtain. This is illustrated in the electrophysiological selectivity data for Ca<sub>v</sub>2.1, Ca<sub>v</sub>2.2, and Ca<sub>v</sub>2.3 at -100 mV, where TROX-1 seems to be ~30-fold selective over Ca<sub>v</sub>2.1 channels but actually shows no true molecular selectivity.

TROX-1 is an orally available, small-molecule Ca<sub>v</sub>2.2 inhibitor with efficacy in a number of animal models and a demonstrated therapeutic window in animals over cardiovascular and neurological side effects (Abbadie et al., 2010). This article provides a detailed characterization of the state- and use-dependent properties of TROX-1. The comprehensive selectivity characterization shows that TROX-1 is a state-dependent inhibitor of all members of the Ca<sub>v</sub>2 subfamily with similar potency when normalized to the degree of inactivation. Together, these data support the idea that a state-dependent Ca<sub>v</sub>2 inhibitor can provide an improved therapeutic window over a relatively state-independent Ca<sub>v</sub>2.2 inhibitor, such as ziconotide (Snutch, 2005; Abbadie et al., 2010). In addition, this article presents the most comprehensive characterization of a small-molecule Cav2 inhibitor to date and should further promote the use of TROX-1 as a benchmark compound. As detailed compound characterizations become available for additional Ca<sub>v</sub>2 inhibitors, our understanding of how state dependence and selectivity influence safety margins and analgesic efficacy will improve. The preclinical profile of TROX-1 suggests a potential future avenue to develop small molecule Ca<sub>v</sub>2.2 blockers for clinical trials. Ultimately, optimizing state dependence and selectivity will be essential to realize the full therapeutic potential of targeting Ca<sub>v</sub>2.2 channels.

#### Acknowledgments

We thank members of the Ion Channel Department, Merck Research Labs, and Dr. Elizabeth Tringham (Zalicus Pharmaceuticals) for helpful discussions.

#### Authorship Contributions

*Participated in research design:* Swensen, Herrington, Bugianesi, Smith, Arneric, Eduljee, Snutch, Duffy, Kaczorowski, and McManus.

*Conducted experiments:* Swensen, Herrington, Bugianesi, Dai, Haedo, Ratliff, Smith, Warren, and Eduljee.

*Contributed new reagents or analytic tools:* Parker, Hoyt, London, and Duffy.

*Performed data analysis:* Swensen, Herrington, Bugianesi, Dai, Haedo, Ratliff, Smith, Warren, Eduljee, and McManus.

*Wrote or contributed to the writing of the manuscript:* Swensen, Herrington, Eduljee, and McManus.

#### References

- Abbadie C, McManus OB, Sun SY, Bugianesi RM, Dai G, Haedo RJ, Herrington JB, Kaczorowski GJ, Smith MM, Swensen AM, et al. (2010) Analgesic effects of a substituted N-triazole oxindole (TROX-1), a state-dependent, voltage-gated calcium channel 2 blocker. *J Pharmacol Exp Ther* **334**:545–555.
- Bean BP (1984) Nitrendipine block of cardiac calcium channels: high-affinity binding to the inactivated state. *Proc Natl Acad Sci USA* **81**:6388–6392.
- Bezprozvanny I, Scheller RH, and Tsien RW (1995) Functional impact of syntaxin on gating of N-type and Q-type calcium channels. *Nature* **378**:623–626.
- Bourinet E, Soong TW, Sutton K, Slaymaker S, Mathews E, Monteil A, Zamponi GW, Nargeot J, and Snutch TP (1999) Splicing of alpha 1A subunit gene generates phenotypic variants of P- and Q-type calcium channels. *Nat Neurosci* **2**:407–415.
- Cizkova D, Marsala J, Lukacova N, Marsala M, Jergova S, Orendacova J, and Yaksh TL (2002) Localization of N-type Ca<sup>2+</sup> channels in the rat spinal cord following chronic constrictive nerve injury. *Exp Brain Res* **147**:456–463.
- Dai G, Haedo RJ, Warren VA, Ratliff KS, Bugianesi RM, Rush A, Williams ME, Herrington J, Smith MM, McManus OB, et al. (2008) A high-throughput assay for

- evaluating state dependence and subtype selectivity of Cav2 calcium channel inhibitors. *Assay Drug Dev Technol* **6**:195–212.
- De Waard M and Campbell KP (1995) Subunit regulation of the neuronal alpha 1A Ca<sup>2+</sup> channel expressed in *Xenopus oocytes*. *J Physiol* **485**:619–634.
- Ebersberger A, Portz S, Meissner W, Schaible HG, and Richter F (2004) Effects of N-, P/Q- and L-type calcium channel blockers on nociceptive neurones of the trigeminal nucleus with input from the dura. *Cephalalgia* **24**:250–261.
- Evans AR, Nicol GD, and Vasko MR (1996) Differential regulation of evoked peptide release by voltage-sensitive calcium channels in rat sensory neurons. *Brain Res* **712**:265–273.
- Feng ZP, Doering CJ, Winkfein RJ, Beedle AM, Spafford JD, and Zamponi GW (2003) Determinants of inhibition of transiently expressed voltage-gated calcium channels by omega-conotoxins GVIA and MVIIA. *J Biol Chem* **278**:20171–20178.
- Gohil K, Bell JR, Ramachandran J, and Miljanich GP (1994) Neuroanatomical distribution of receptors for a novel voltage-sensitive calcium-channel antagonist, SNX-230 ( $\omega$ -conopeptide MVIIIC). *Brain Res* **653**:258–266.
- Hans M, Urrutia A, Deal C, Brust PF, Stauderman K, Ellis SB, Harpold MM, Johnson EC, and Williams ME (1999) Structural elements in domain IV that influence biophysical and pharmacological properties of human alpha1A-containing high-voltage-activated calcium channels. *Biophys J* **76**:1384–1400.
- Hatakeyama S, Wakamori M, Ino M, Miyamoto N, Takahashi E, Yoshinaga T, Sawada K, Imoto K, Tanaka I, Yoshizawa T, et al. (2001) Differential nociceptive responses in mice lacking the  $\alpha 1B$  subunit of N-type Ca<sup>2+</sup> channels. *NeuroReport* **12**:2423–2427.
- Kim C, Jun K, Lee T, Kim SS, McEnery MW, Chin H, Kim HL, Park JM, Kim DK, Jung SJ, et al. (2001) Altered nociceptive response in mice deficient in the alpha1B subunit of the voltage-dependent calcium channel. *Mol Cell Neurosci* **18**:235–245.
- Kiyonaka S, Wakamori M, Miki T, Uruu Y, Nonaka M, Bito H, Beedle AM, Mori E, Hara Y, De Waard M, et al. (2007) RIM1 confers sustained activity and neurotransmitter vesicle anchoring to presynaptic Ca<sup>2+</sup> channels. *Nat Neurosci* **10**:691–701.
- Knight YE, Bartsch T, Kaube H, and Goadsby PJ (2002) P/Q-type calcium-channel blockade in the periaqueductal gray facilitates trigeminal nociception: a functional genetic link for migraine? *J Neurosci* **22**:RC213.
- Luvisetto S, Marinelli S, Panasiti MS, D'Amato FR, Fletcher CF, Pavone F, and Pietrobon D (2006) Pain sensitivity in mice lacking the Ca(v)2.1alpha1 subunit of P/Q-type Ca<sup>2+</sup> channels. *Neuroscience* **142**:823–832.
- Malmberg AB and Yaksh TL (1995) Effect of continuous intrathecal infusion of omega-conopeptides, N-type calcium-channel blockers, on behavior and antinociception in the formalin and hot-plate tests in rats. *Pain* **60**:83–90.
- Matsuda Y, Saegusa H, Zong S, Noda T, and Tanabe T (2001) Mice lacking Ca(v)2.3 (alpha1E) calcium channel exhibit hyperglycemia. *Biochem Biophys Res Commun* **289**:791–795.
- McDonough SI and Bean BP (1998) Mibefradil inhibition of T-type calcium channels in cerebellar purkinje neurons. *Mol Pharmacol* **54**:1080–1087.
- McGivern JG and McDonough SI (2004) Voltage-gated calcium channels as targets for the treatment of chronic pain. *Curr Drug Targets CNS Neurol Disord* **3**:457–478.
- Miljanich GP (2004) Ziconotide: neuronal calcium channel blocker for treating severe chronic pain. *Curr Med Chem* **11**:3029–3040.
- Périer F, Radeke CM, and Vandenberg CA (1994) Primary structure and characterization of a small-conductance inwardly rectifying potassium channel from human hippocampus. *Proc Natl Acad Sci USA* **91**:6240–6244.
- Pietrobon D (2005) Function and dysfunction of synaptic calcium channels: insights from mouse models. *Curr Opin Neurobiol* **15**:257–265.
- Saegusa H, Kurihara T, Zong S, Kazuno A, Matsuda Y, Nonaka T, Han W, Toriyama H, and Tanabe T (2001) Suppression of inflammatory and neuropathic pain symptoms in mice lacking the N-type Ca<sup>2+</sup> channel. *EMBO J* **20**:2349–2356.
- Saegusa H, Kurihara T, Zong S, Minowa O, Kazuno A, Han W, Matsuda Y, Yamanaka H, Osanai M, Noda T, et al. (2000) Altered pain responses in mice lacking alpha 1E subunit of the voltage-dependent Ca<sup>2+</sup> channel. *Proc Natl Acad Sci USA* **97**:6132–6137.
- Scott DA, Wright CE, and Angus JA (2002) Actions of intrathecal omega-conotoxins CVID, GVIA, MVIIA, and morphine in acute and neuropathic pain in the rat. *Eur J Pharmacol* **451**:279–286.
- Snutch TP (2005) Targeting chronic and neuropathic pain: the N-type calcium channel comes of age. *NeuroRx* **2**:662–670.
- Staats PS, Yearwood T, Charapata SG, Presley RW, Wallace MS, Byas-Smith M, Fisher R, Bryce DA, Mangieri EA, Luther RR, et al. (2004) Intrathecal ziconotide in the treatment of refractory pain in patients with cancer or AIDS: a randomized controlled trial. *JAMA* **291**:63–70.
- Stocker JW, Nadasdi L, Aldrich RW, and Tsien RW (1997) Preferential interaction of omega-conotoxins with inactivated N-type Ca<sup>2+</sup> channels. *J Neurosci* **17**:3002–3013.
- Thaler C, Gray AC, and Lipscombe D (2004) Cumulative inactivation of N-type CaV2.2 calcium channels modified by alternative splicing. *Proc Natl Acad Sci USA* **101**:5675–5679.
- Westenbroek RE, Hoskins L, and Catterall WA (1998) Localization of Ca<sup>2+</sup> channel subtypes on rat spinal motor neurons, interneurons, and nerve terminals. *J Neurosci* **18**:6319–6330.
- Williams ME, Brust PF, Feldman DH, Patthi S, Simerson S, Maroufi A, McCue AF, Velichelebi G, Ellis SB, and Harpold MM (2002) Structure and functional expression of an omega-conotoxin-sensitive human N-type calcium channel. *Science* **257**:389–395.
- Williams ME, Marubio LM, Deal CR, Hans M, Brust PF, Philipson LH, Miller RJ, Johnson EC, Harpold MM, and Ellis SB (1994) Structure and functional characterization of neuronal alpha 1E calcium channel subtypes. *J Biol Chem* **269**:22347–22357.
- Wilson SM, Toth PT, Oh SB, Gillard SE, Volsen S, Ren D, Philipson LH, Lee EC, Fletcher CF, Tessarollo L, et al. (2000) The status of voltage-dependent calcium channels in alpha 1E knock-out mice. *J Neurosci* **20**:8566–8571.
- Winquist RJ, Pan JQ, and Gribkoff VK (2005) Use-dependent blockade of Cav2.2 voltage-gated calcium channels for neuropathic pain. *Biochem Pharmacol* **70**:489–499.
- Yamamoto T and Takahara A (2009) Recent updates of N-type calcium channel blockers with therapeutic potential for neuropathic pain and stroke. *Curr Top Med Chem* **9**:377–395.
- Zamponi GW, Feng ZP, Zhang L, Pajouhesh H, Ding Y, Belardetti F, Pajouhesh H, Dolphin D, Mitscher LA, and Snutch TP (2009) Scaffold-based design and synthesis of potent N-type calcium channel blockers. *Bioorg Med Chem Lett* **19**:6467–6472.
- Zhang S, Su R, Zhang C, Liu X, Li J, and Zheng J (2008) C101, a novel 4-aminopiperidine derivative selectively blocks N-type calcium channels. *Eur J Pharmacol* **587**:42–47.
- Zhong H, Yokoyama CT, Scheuer T, and Catterall WA (1999) Reciprocal regulation of P/Q-type Ca<sup>2+</sup> channels by SNAP-25, syntaxin and synaptotagmin. *Nat Neurosci* **2**:939–941.

**Address correspondence to:** Owen B. McManus, Johns Hopkins Ion Channel Center, Department of Neuroscience, Johns Hopkins School of Medicine, 733 North Broadway, Baltimore, MD 21205. E-mail: owen\_mcmanus@jhmi.edu